

Supporting Information

Qualitative Effect of Polymerization Rate on the Nanoparticle Dispersion in Poly(methyl methacrylate)/Silica Nanocomposite Films

Che-Yi Chu^{1*}, Yen-Cheng Li², Guang-Way Jang,² Ying-Chih Pu,³ Meng-Zhe Chen¹
and Pei-Yin Chen²

¹Department of Chemical Engineering, National Chung Hsing University, Taichung 402, Taiwan

²Material and Chemical Research Laboratories, Industrial Technology Research Institute, Hsin-Chu 31040, Taiwan

³Department of Materials Science, National University of Tainan, Tainan 70005, Taiwan

*To whom correspondence should be addressed (C.-Y. Chu: cychu0123@dragon.nchu.edu.tw)

The Supporting Information contains the following information and figures.

1. Description of the derivations of equations used for model fitting in this study.
2. TGA curve of M-SiO₂ nanoparticles (**Figure S1**)
3. FTIR spectrum of M-SiO₂ nanoparticles (**Figure S2**)
4. TGA curve of PMMA/M-SiO₂ nanocomposites (**Figure S3**)
5. SAXS profile with minimum q down to 0.0024 \AA^{-1} of PMMA/M-SiO₂ nanocomposites (**Figure S4**)
6. SAXS profiles of PMMA/M-SiO₂ nanocomposites prepared at different polymerization temperatures (**Figure S5**)
7. 3D TEM images of PMMA/M-SiO₂ nanocomposites prepared at different AIBN concentrations (**Figure S6**)
8. GPC curves of neat PMMA polymerized at different AIBN concentrations (**Figure S7**)
9. Fits of SAXS profiles of PMMA/M-SiO₂ nanocomposites prepared at different AIBN concentrations (**Figure S8**)

Equations Used for Model Fitting in this Study.⁴²

The differential scattering cross section $d\Sigma(q)/d\Omega$ for primary spherical SiO₂ nanoparticles distributed over an infinitely larger PMMA matrix is given by the Zernike-Prins (ZP) equation,⁴³

$$\frac{d\Sigma(q)}{d\Omega} = P(q)S(q) \quad (1)$$

where $P(q)$ is the spherical form factor of the SiO₂ nanoparticles, $S(q)$ is the ZP structure factor given by

$$S(q) = N \left[1 + n \int_0^\infty g(r) \frac{\sin qr}{qr} 4\pi r^2 dr \right] \quad (2)$$

where N is the total number of the SiO₂ nanoparticles in the infinitely large PMMA space, $n = N/V_{ir}$ with V_{ir} being the irradiated volume with the incident beam, and $g(r)$ is the radial distribution function of the SiO₂ nanoparticles. Since $g(r) - 1 = h(r)$, where $h(r)$ is the total correlation function,⁴⁴ eq (2) can be rewritten as

$$S(q) = N[\pi^3 n \delta(q) + S_{ZP}(q)] \quad (3)$$

and

$$S_{ZP}(q) = 1 + n \int_0^\infty h(r) \frac{\sin qr}{qr} 4\pi r^2 dr \quad (4)$$

where $\delta(q)$ is the Dirac's delta function. $h(r)$ can be further expressed in terms of the direct correlation function $C(r)$ via the Ornstein-Zernike (OZ) equation,⁴⁴ $h(r) = C(r) + nC(r) * h(r)$, and its Fourier transform gives

$$h(q) = C(q) + nC(q) h(q) \quad (5)$$

where

$$h(q) \equiv \int_0^\infty h(r) \frac{\sin qr}{qr} 4\pi r^2 dr \quad (6)$$

$$C(q) \equiv \int_0^\infty C(r) \frac{\sin qr}{qr} 4\pi r^2 dr \quad (7)$$

Thus, substituting eq (5) into eq (4) leads to

$$S_{ZP}(q) = \frac{1}{1-nC(q)} \quad (8)$$

In the case of the hard-sphere potential with the Percus-Yevick (PY) closure

(hard-sphere model) for the polydisperse SiO₂ nanoparticles:⁴²

Considering the scattering theory based on the Percus-Yevick (PY) equation given by⁴⁵

$$C(r) = g(r)\{1 - \exp[u(r)/k_B T]\} \quad (9)$$

where $u(r)$ is the potential energy for the interparticle interaction and k_B is the Boltzmann constant, the relationship among $C(r)$, $g(r)$ and $u(r)$ in eq (9) can be applied for computing the hard-core repulsive potential between SiO₂ nanoparticles.

The analytical solution for $C(r)$ has been solved by Wertheim,⁴⁶ leading to $u(r)$ given by

$$u(r) = \begin{cases} +\infty, & \text{for } r < 2R_p \\ 0, & \text{for } r \geq 2R_p \end{cases} \quad (10)$$

where R_p is the effective radius of the sphere (which hereafter denotes the effective radius of the SiO₂ nanoparticles). The result for $C(r)$ is given by

$$C(r) = \begin{cases} -(\alpha + \beta s + \gamma s^3)/(1 - \phi)^4, & \text{for } s \leq 1 \\ 0, & \text{for } s > 1 \end{cases} \quad (11)$$

where $s \equiv r/(2R_p)$ denotes the reduced distance and $\phi \equiv n(4\pi R_p^3/3)$ is the effective volume fraction. The coefficients α , β and γ are given by $(1 + 2\phi)^2$, $-6\phi \left[1 + \left(\frac{\phi}{2}\right)\right]^2$ and $\left(\frac{1}{2}\right)\phi(1 + 2\phi)^2$, respectively. The Fourier transform of $C(r)$ gives $C(q)$ which is evaluated to give $S_{ZP}(q)$ in eq (8),⁴⁷ thus leading to

$$S_{ZP}(q) = [1 - nC(q)]^{-1} = \{1 + 24\phi[G(A)/A]\}^{-1} \quad (12)$$

where

$$G(A) = \frac{\alpha}{A^2}(\sin A - A \cos A) + \frac{\beta}{A^3}[2A \sin A + (2 - A^2) \cos A - 2] \\ + \frac{\gamma}{A^5}\{-A^4 \cos A + 4[(3A^2 - 6) \cos A + (A^3 - 6A) \sin A + 6]\} \\ A = 2qR_p \quad (13)$$

The combination of eq (1), eq (3), eq (11), eq (12), and eq (13) is the so-called hard-sphere model considering the hard-core potential with the PY closure.

The spherical form factor of the SiO₂ nanoparticle can be given by

$$P(q) = \Delta\rho^2 V_p^2 \Phi^2(qR_p) \quad (14)$$

and

$$\Phi(qR_p) = \frac{3(\sin qR_p - qR_p \cos qR_p)}{(qR_p)^3} \quad (15)$$

where $\Delta\rho$ is the electron density difference between the SiO₂ nanoparticle and the PMMA matrix phase and $V_p = \frac{4\pi R_p^3}{3}$. From eq (1), eq (3), eq (11), eq (12), eq (13), eq (14), and eq (15),

$$\frac{d\Sigma(q)}{d\Omega} = n\Delta\rho^2 V_p^2 \Phi^2(qR_p) S_{ZP}(q) \quad (16)$$

Now considering the effect of the polydispersity on $\frac{d\Sigma(q)}{d\Omega}$ in eq (16), it is rewritten by

$$\frac{d\Sigma(q)}{d\Omega} = n\Delta\rho^2 \langle V_p^2 \Phi^2(q; R_p) S_{ZP}(q; R_p) \rangle \quad (17)$$

where $\langle \rangle$ denotes the average with respect to the distribution of R_p and $S_{ZP}(q; R_p)$ depends on the size distribution of R_p through the radial distribution function of the nanoparticles. Here, the ‘‘average structure factor approximation’’⁴⁸ is adopted to introduce $S_{ZP}(q; R_{p,av})$ representing the ZP structure factor for the monodisperse sphere having the average size $R_{p,av}$, therefore, eq (17) can be rewritten as

$$\frac{d\Sigma(q)}{d\Omega} = n\Delta\rho^2 \langle V_p^2 \Phi^2(q; R_p) \rangle S_{ZP}(q; R_{p,av}) \quad (18)$$

and

$$\langle V_p^2 \Phi^2(q; R_p) \rangle = \int_0^\infty P_N(R_p) \left(\frac{4\pi R_p^3}{3}\right)^2 \Phi^2(q; R_p) dR_p \quad (19)$$

$$R_{p,av}^3 \equiv \int_0^\infty P_N(R_p) R_p^3 dR_p \quad (20)$$

where $P_N(R_p)$ is the normalized distribution function for the number of the nanoparticles with R_p radius. It is assumed that $P_N(R_p)$ is given by Schultz distribution as⁴⁹

$$P_N(R_p) = (Z + 1)^{Z+1} \left(\frac{R_p}{\langle R_p \rangle}\right)^Z \left\{ \frac{\exp[-(Z+1)\left(\frac{R_p}{\langle R_p \rangle}\right)]}{\langle R_p \rangle \Gamma(Z+1)} \right\} \quad (21)$$

where $\langle R_p \rangle$ is the number-average radius of the nanoparticles, $Z = \left(\frac{1}{P_p^2}\right) - 1$ is the polydispersity of the nanoparticles, $P_p = \frac{\sigma_p}{\langle R_p \rangle}$ with σ_p^2 being the variance of the distribution, and $\Gamma(Z)$ is the gamma function.

As derived above, the hard-sphere potential with the PY closure (i.e., the hard-sphere model) for the scattering from polydisperse SiO₂ nanoparticles is given by eqs (17) to (21). These equations were used to carry out the model fitting for the SAXS profile of the PMMA/M-SiO₂ nanocomposite prepared at 0.01 wt% AIBN, as can be seen in Figure 6 and Figure S8.

In the case of the screened Coulomb potential with the Mean Spherical Approximation (MSA) closure for the polydisperse SiO₂ nanoparticles:

However, when considering the scattering theory based on the Mean Spherical Approximation (MSA) equation given by⁵⁰

$$\begin{cases} C(r) = -\beta u(r), & \text{for } r > 2R_p \\ h(r) = -1, & \text{for } r < 2R_p \end{cases} \quad (22)$$

where $u(r)$ is the Coulomb interaction potential given by

$$u(r) = \pi \varepsilon_0 \varepsilon (2R_p)^2 \Psi_0^2 \frac{\exp[-\kappa(r-2R_p)]}{r} \quad (23)$$

and

$$\Psi_0 = \frac{z}{\pi \varepsilon_0 \varepsilon [2 + \kappa(2R_p)]} \quad (24)$$

where ε_0 is the permittivity of free vacuum, ε is the dielectric constant, Ψ_0 is the macroion surface interaction potential, κ is the Debye-Hückel inverse screening length, and z is the charge number of the nanoparticle. The Debye-Hückel inverse screening length is expressed as

$$\kappa = \left(\frac{e^2 z n}{k_B T} \right)^{\frac{1}{2}} \quad (25)$$

where e is the electron charge and ze is the charge on the nanoparticle surface.

Besides, the contact potential for $r = 2R_p$ is given by

$$\gamma' \exp[-\kappa(2R_p)] = \frac{\pi\epsilon_0\epsilon\Psi_0^2}{k_B T} \quad (26)$$

The relationship among $C(r)$, $h(r)$ and $u(r)$ in eq (22) can be applied for computing the screened Coulomb potential between SiO_2 nanoparticles. On the basis of the MSA closure given by eq (22), the analytical solution for $C(r)$ has been solved,⁵⁰ leading to

$$C(r) = \begin{cases} A' + B's + \frac{1}{2}A'\phi s^3 + \frac{C'\sinh[\kappa(2R_p)s]}{s} + \frac{F'(\cosh[\kappa(2R_p)s]-1)}{s}, & \text{for } s < 1 \\ \frac{-\gamma'\exp[-\kappa(2R_p)s]}{s}, & \text{for } s > 1 \end{cases} \quad (27)$$

where the expressions for the constants A' , B' , C' , and F' are too lengthy to reproduce here but can be found in the original literature.⁵⁰ The Fourier transform of $C(r)$ gives $C(q)$ which is evaluated to give $S_{ZP}(q)$ in eq (8), thereby leading to

$$S_{ZP}(q) = [1 - nC(q)]^{-1} = \{1 - 24\phi[G'(A)]\}^{-1} \quad (28)$$

where

$$\begin{aligned}
G'(A) = & \frac{A'(\sin A - A \cos A)}{A^3} + \frac{B'[(\frac{2}{A} - A) \cos A + 2 \sin A - \frac{2}{A}]}{A^3} \\
& + \frac{\phi A'[\frac{24}{A^3} + 4(1 - \frac{6}{A^2}) \sin A - A(1 - \frac{12}{A^2} + \frac{24}{A^4}) \cos A]}{2A^3} \\
& + \frac{C'\{\kappa(2R_p) \cosh[\kappa(2R_p)] \sin A - A \sinh[\kappa(2R_p)] \cos A\}}{A\{A^2 + [\kappa(2R_p)]^2\}} \\
& + \frac{F'\{\kappa(2R_p) \sinh[\kappa(2R_p)] \sin A - A \cosh[\kappa(2R_p)] \cos A - A\}}{A\{A^2 + [\kappa(2R_p)]^2\}} \\
& + \frac{F'(\cos A - 1)}{A^2} \\
& - \frac{\gamma'[\kappa(2R_p) \sin A + A \cos A] \exp[-\kappa(2R_p)]}{A\{A^2 + [\kappa(2R_p)]^2\}} \\
& A = 2qR_p \quad (29)
\end{aligned}$$

The combination of eq (1), eq (3), eq (27), eq (28), and eq (29) is the model considering the screened Coulomb potential with the MSA closure.

Again, the combination of eq (1), eq (3), eq (14), eq (15), eq (27), eq (28), and eq (29) leads to eq (16). Let us also consider the effect of the polydispersity on $\frac{d\Sigma(q)}{d\Omega}$ in eq (16) and adopt the ‘‘average structure factor approximation’’,⁴⁸ thus leading to eq (18), eq (19), and eq (20) through eq (17). In addition, it is assumed that the normalized distribution function for the number of the nanoparticles is given by Schultz distribution in eq (21).⁴⁹

As derived above, the screened Coulomb potential with the MSA closure for the scattering from polydisperse SiO₂ nanoparticles is given by eqs (17) to (21). These equations were used to carry out the model fitting for the SAXS profile of the aqueous

dispersion of 15.5 wt% SiO₂ nanoparticles, as can be seen in Figure 2.

Polydisperse spherical form factor:

It is noted that the spherical form factor of the SiO₂ nanoparticle can be given by eq (14) and eq (15). Let us consider the effect of the polydispersity on $P(q)$ in eq (14), it is rewritten by

$$P(q) = \Delta\rho^2 \langle V_p^2 \Phi^2(q; R_p) \rangle \quad (30)$$

where $\Delta\rho$ is the electron density difference between the SiO₂ nanoparticle and the aqueous solvent. Again, it is assumed that the normalized distribution function for the number of the nanoparticles is given by Schultz distribution in eq (21).⁴⁹ Therefore, the polydisperse spherical form factor for the scattering from polydisperse SiO₂ nanoparticles is given by eq (30). This equation was used to carry out the model fitting for the SAXS profile of the aqueous dispersion of 0.1 wt% SiO₂ nanoparticles, as can be seen in Figure 1.

Polydisperse core-shell spherical form factor:

The core-shell spherical form factor of the M-SiO₂ nanoparticles can be given by⁵¹

$$P(q) = \frac{1}{V_{p+s}} \Phi^2(qR_p, qR_{p+s}) \quad (31)$$

and

$$\Phi(qR_p, qR_{p+s}) = \frac{3V_p(\rho_p - \rho_s)j_1(qR_p)}{qR_p} + \frac{3V_s(\rho_s - \rho_{\text{soln}})j_2(qR_{p+s})}{qR_{p+s}} \quad (32)$$

$$j_1(qR_p) = \frac{\sin(qR_p) - qR_p \cos(qR_p)}{(qR_p)^2} \quad (33)$$

$$j_2(qR_{p+s}) = \frac{\sin(qR_{p+s}) - qR_{p+s} \cos(qR_{p+s})}{(qR_{p+s})^2} \quad (34)$$

where $R_{p+s} = R_p + t_s$ with t_s being the MSMA shell thickness, $V_{p+s} = \frac{4\pi(R_{p+s})^3}{3}$, V_s is the volume of the MSMA shell, $(\rho_p - \rho_s)$ is the electron density difference between the SiO₂ nanoparticle and the MSMA silane, and $(\rho_s - \rho_{\text{solv}})$ is the electron density difference between the MSMA silane and the MMA monomer. Let us consider the effect of the polydispersity on $P(q)$ in eq (31), and eq (31) is rewritten by

$$P(q) = \left\langle \frac{1}{V_{p+s}} \Phi^2(q; R_p, q; R_{p+s}) \right\rangle \quad (35)$$

where $\langle \rangle$ denotes the average with respect to the distribution of R_p while t_s is held constant. It is again assumed that the normalized distribution function for the number of the nanoparticles is given by Schultz distribution in eq (21).⁴⁹ Consequently, the polydisperse core-shell spherical form factor for the scattering from polydisperse M-SiO₂ nanoparticles is given by eq (35). This equation was used to carry out the model fitting for the SAXS profile of the MMA dispersion of 15.5 wt% M-SiO₂ nanoparticles, as can be seen in Figure 2.

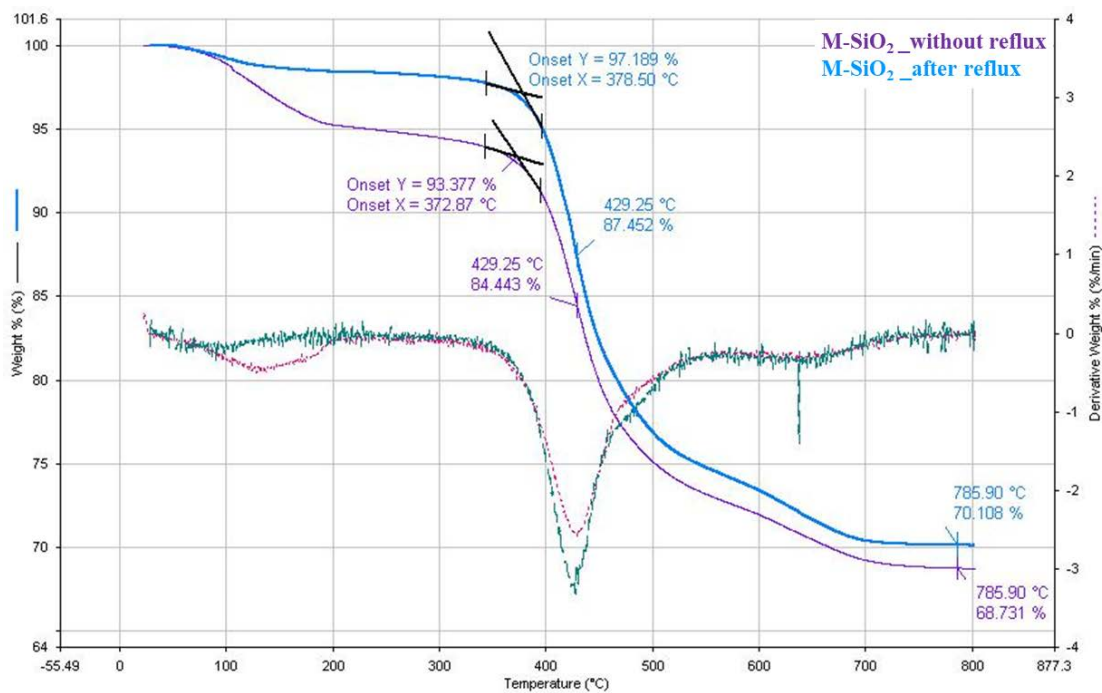


Figure S1. TGA curve (conducted in an oxidative environment of air) of the M-SiO₂ nanoparticles (see the curve labelled by M-SiO₂_after reflux), in which the weight percentage of the tethered MSMA silanes on each M-SiO₂ nanoparticle was about

27.9 wt% ($= \frac{97.189 \text{ wt\%} - 70.108 \text{ wt\%}}{97.189 \text{ wt\%}} \times 100 \text{ wt\%}$) and that of SiO₂ was about 72.1 wt%.

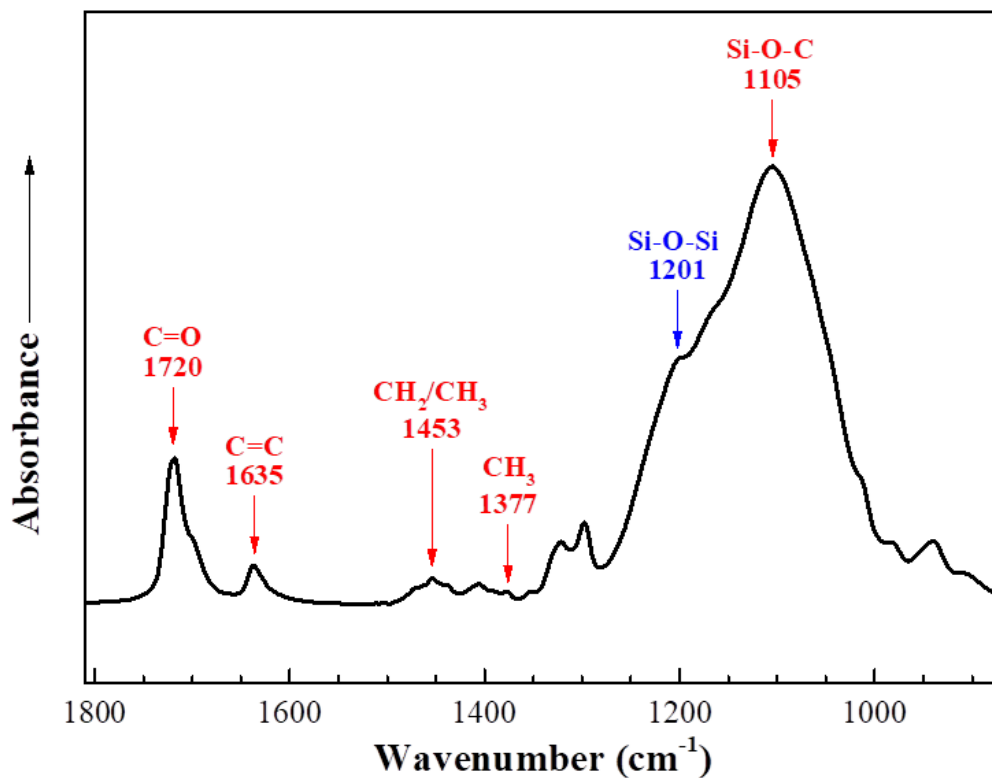


Figure S2. FTIR spectrum of the M-SiO₂ nanoparticles, in which “C=O (at 1720 cm⁻¹)”, “C=C (at 1635 cm⁻¹)”, “CH₂ (at 1453 cm⁻¹)”, “CH₃ (at 1453 and 1377 cm⁻¹)” and “Si-O-C (at 1105 cm⁻¹)” denote the signals of bands from the functional groups in [3-(methacryloyloxy)propyl]trimethoxysilane.

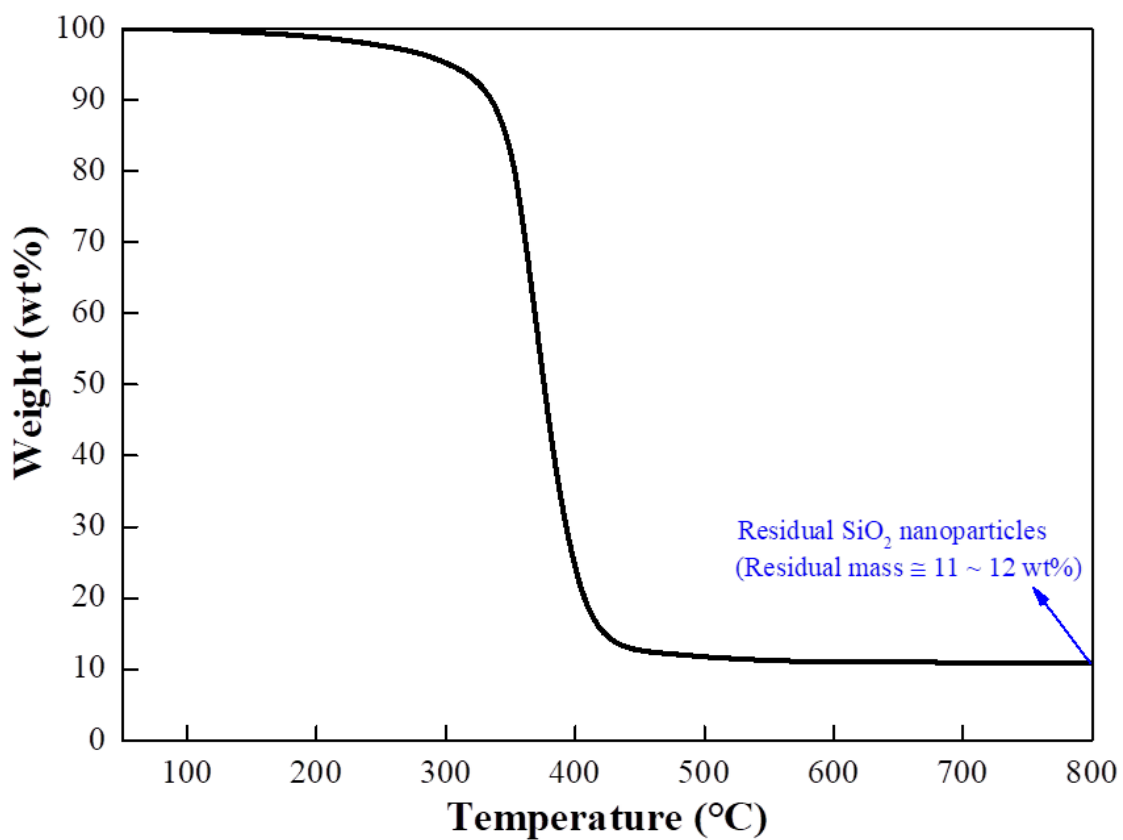


Figure S3. TGA curve (conducted in an oxidative environment of air) of the PMMA/M-SiO₂ nanocomposite collected after the nanocomposite has been dehydrated at 100 °C for 3 h. The weight percentage of the residual SiO₂ nanoparticles was ca. 11 ~ 12 wt%.

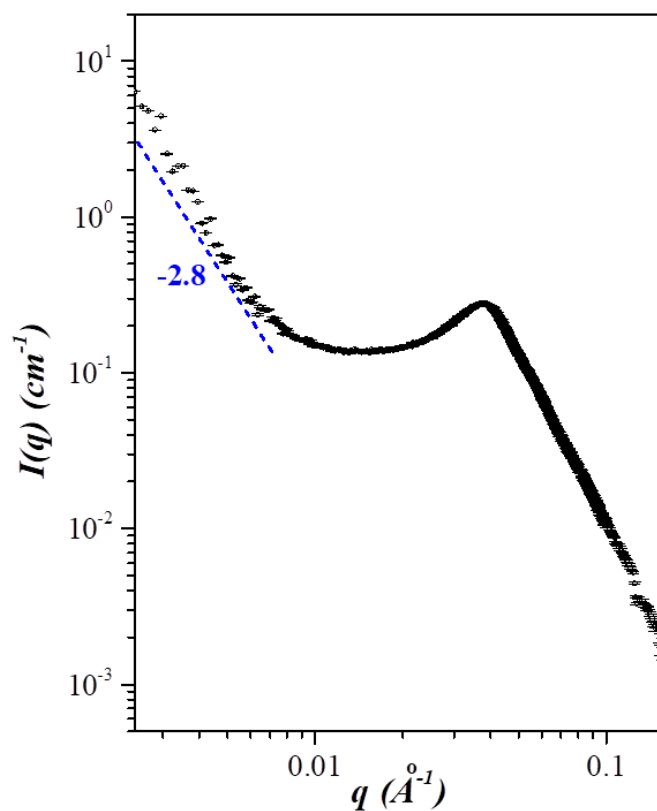


Figure S4. SAXS profile (with the reliable q_{\min} down to 0.0024 \AA^{-1}) of the PMMA/M-SiO₂ nanocomposite collected after the precursor solution, i.e., 15.5 wt% M-SiO₂ dispersed in MMA medium with 0.01 wt% AIBN initiator, has been pre-polymerized at 75 °C for 3 h followed by a polymerization at 100 °C for 3 h.

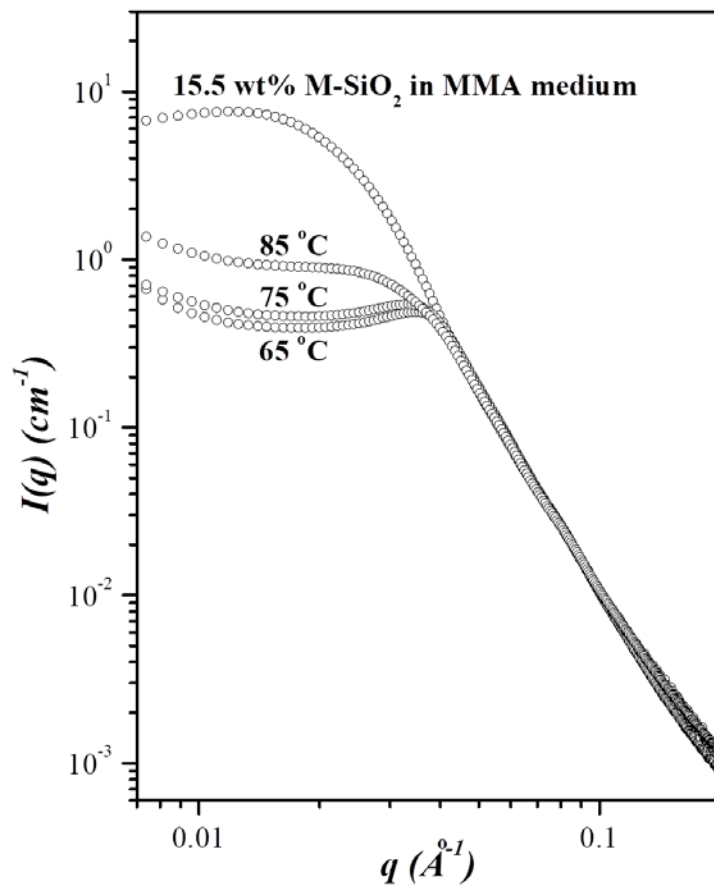


Figure S5. SAXS profiles of the PMMA/M-SiO₂ nanocomposites collected after the precursor solution (i.e., 15.5 wt% M-SiO₂ dispersed in MMA medium with 0.1 wt% AIBN) has been respectively pre-polymerized at the different prescribed temperatures for 3 h followed by a polymerization at 100 °C for 3 h.

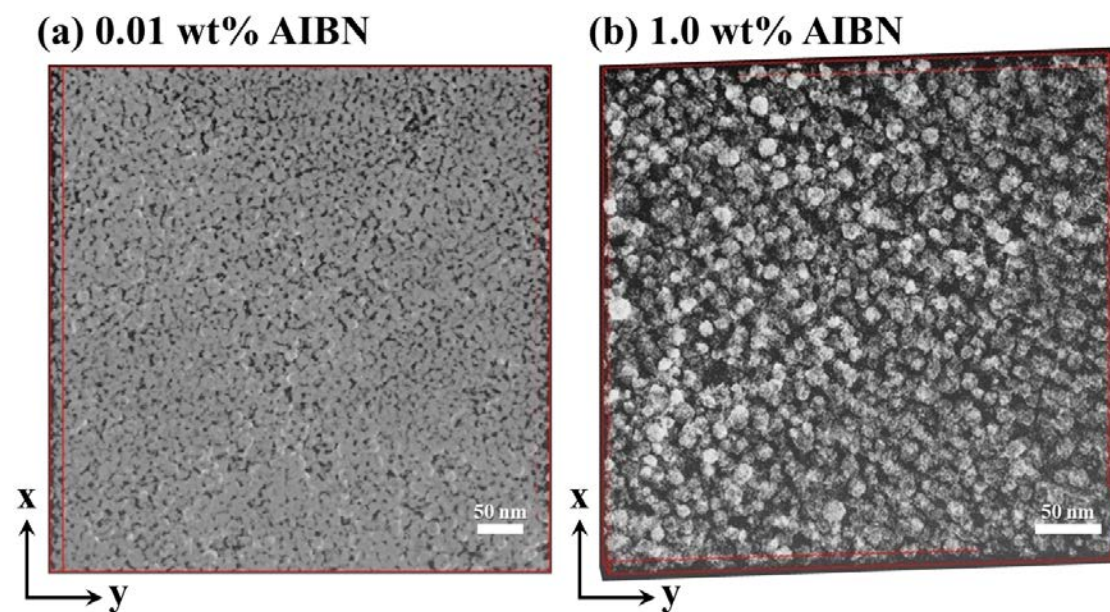


Figure S6. 3D TEM images of the nanoparticle dispersion in the PMMA/M-SiO₂ nanocomposites prepared at (a) 0.01 wt% AIBN and (b) 1.0 wt% AIBN, respectively. The SiO₂ nanoparticles appear as the bright region in the image while PMMA matrix corresponds to the dark region.

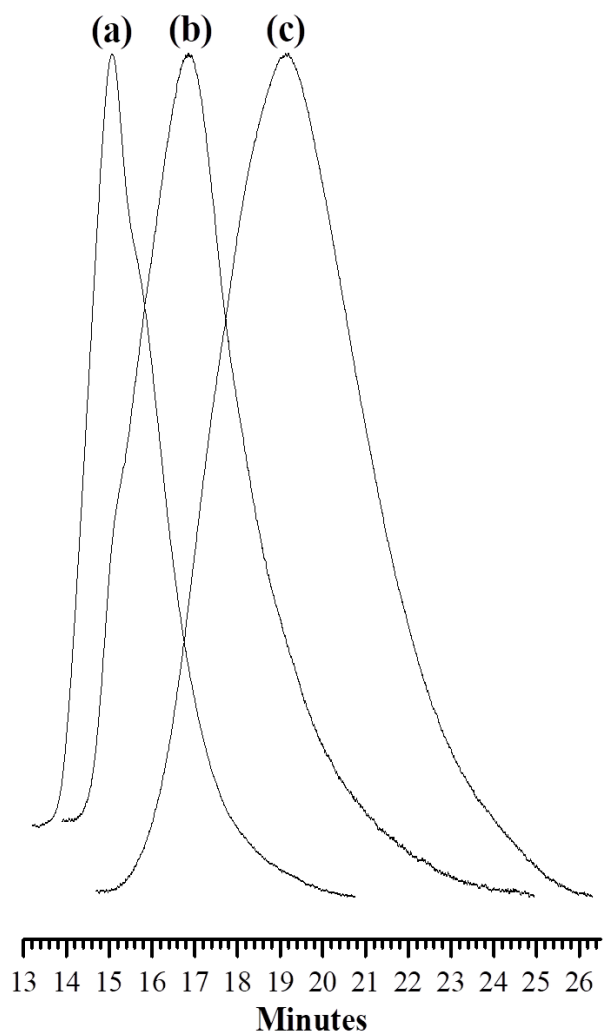


Figure S7. GPC curves of the neat PMMA polymerized with the addition of (a) 0.01 wt% AIBN ($M_w = 1179$ kg/mol, $M_w/M_n = 2.52$), (b) 0.1 wt% AIBN ($M_w = 272$ kg/mol, $M_w/M_n = 1.76$), and (c) 1.0 wt% AIBN ($M_w = 73$ kg/mol, $M_w/M_n = 1.24$) (solvent: tetrahydrofuran; temperature: 50 °C).

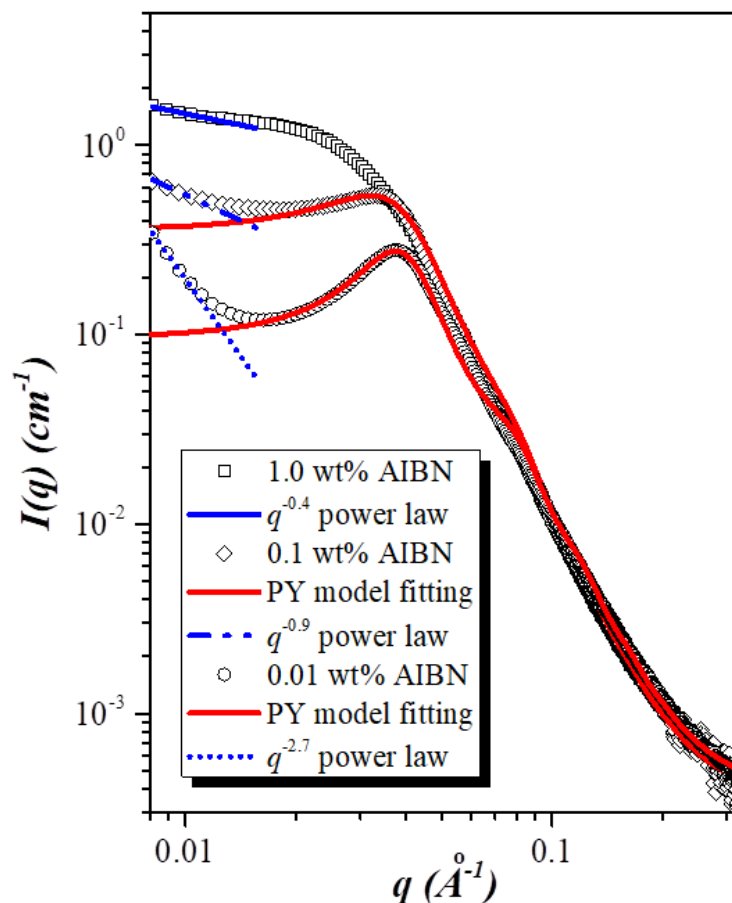


Figure S8. The fits of the SAXS profiles of the PMMA/M-SiO₂ nanocomposites prepared at 0.01, 0.1 and 1.0 wt% AIBN by PY structure factor (the red solid curves) to resolve the repulsive interaction peak associated with the hard-sphere potential between M-SiO₂ nanoparticles within the cluster. The $q^{-2.7}$, $q^{-0.9}$ or $q^{-0.4}$ power law dependence of the scattering intensities in the low- q region for the nanocomposites prepared at 0.01, 0.1 and 1.0 wt% AIBN are represented by the blue dashed line, blue dashed dot line and blue solid line, respectively.